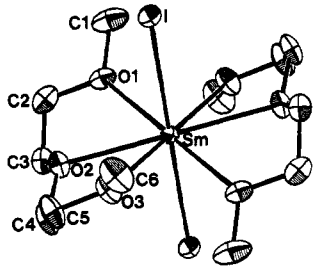

Figure 2. ORTEP drawing of **2**.

Table IV. Positional Parameters and Their Estimated Standard Deviations[a]

atom	*x*	*y*	*z*	*B*, Å^2
		A. Compound **1**		
Sm	0.10866 (4)	0.000	0.333	3.801 (9)
I1	0.000	−0.25167 (5)	0.167	5.19 (2)
I2	0.000	0.13855 (6)	0.167	8.17 (3)
N	0.3320 (7)	0.0883 (8)	0.2282 (7)	8.5 (2)
C1	0.4018 (8)	0.0721 (8)	0.1681 (8)	6.3 (2)
C2	0.4896 (7)	0.0548 (9)	0.0954 (7)	7.2 (2)
C3	0.609 (1)	0.074 (2)	0.150 (1)	19.2 (6)
C4	0.531 (1)	0.150 (2)	0.000 (1)	16.1 (5)
C5	0.412 (1)	−0.078 (2)	0.041 (2)	21.8 (5)
		B. Compound **2**		
Sm	0.000	0.000	0.000	3.060 (9)
I	0.19296 (7)	0.27325 (5)	−0.04404 (4)	5.53 (1)
O1	−0.1994 (6)	0.1836 (6)	0.0584 (4)	5.9 (1)
O2	0.0120 (6)	0.0463 (6)	0.2033 (4)	5.3 (1)
O3	0.2669 (6)	−0.0473 (6)	0.1516 (4)	5.8 (1)
C1	−0.258 (1)	0.301 (1)	−0.001 (1)	9.8 (3)
C2	−0.202 (1)	0.1949 (9)	0.1677 (7)	6.6 (2)
C3	−0.1415 (9)	0.0668 (9)	0.2209 (6)	5.7 (2)
C4	0.101 (1)	−0.058 (1)	0.2678 (5)	6.5 (2)
C5	0.267((1)	−0.040 (1)	0.2587 (8)	7.5 (3)
C6	0.423 (1)	−0.019 (1)	0.135 (1)	8.9 (3)
H1A	−0.301 (7)	0.337 (7)	−0.054 (5)	*
H1B	−0.187 (7)	0.376 (6)	0.038 (5)	*
H1C	−0.396 (8)	0.292 (7)	0.027 (5)	*
H2A	−0.326 (8)	0.239 (7)	0.168 (5)	*
H2B	−0.133 (9)	0.260 (7)	0.211 (5)	*
H3A	−0.108 (8)	0.098 (7)	0.319 (5)	*
H3B	−0.207 (9)	−0.010 (7)	0.199 (6)	*
H4A	0.046 (8)	−0.182 (7)	0.239 (5)	*
H4B	0.106 (8)	−0.070 (7)	0.329 (5)	*
H5A	0.315 (9)	0.014 (7)	0.298 (6)	*
H5B	0.323 (8)	−0.123 (6)	0.293 (5)	*
H6A	0.505 (8)	−0.103 (7)	0.146 (5)	*
H6B	0.463 (9)	0.030 (7)	0.207 (5)	*
H6C	0.417 (9)	0.002 (7)	0.062 (6)	*

[a] Asterisks indicate that the atoms were refined isotropically. Anisotropically refined atoms are given in the form of the isotropic equivalent thermal parameter defined as $^4/_3[a^2\beta_{11} + b^2\beta_{22} + c^2\beta_{33} + ab(\cos\gamma)\beta_{12} + ac(\cos\beta)\beta_{13} + bc(\cos\alpha)\beta_{23}]$.

The standard deviation of an observation of unit weight was 1.61 (1.58 for **2**). The highest peak in the final difference Fourier had a height of 1.92 (17) e/Å^3 (1.13 (12) e/Å^3 for **2**).[18] Plots of $\sum w(|F_o| - |F_c|)^2$ vs. $|F_c|$, reflection order in data collection, $(\sin\theta)/\lambda$, and various classes of indices showed no unusual trends.

The bond distances and bond angles for **1** and **2** are given in Tables II and III, respectively. The positional parameters are given in Table IV.

Acknowledgment. Support of this research through a grant from the National Science Foundation (CHE-8312380) is gratefully acknowledged.

Registry No. **1**, 97316-33-1; **2**, 97316-34-2.

Supplementary Material Available: Tables of thermal parameters and structure factors for **1** and **2** (21 pages). Ordering information is given on any current masthead page.

(18) Cruickshank, D. W. J. *Acta Crystallogr.* **1949**, *2*, 154.

Contribution from the Instituto de Química, Universidade de São Paulo, São Paulo, SP, Brazil

Basicity Constants of Iron(II) and Ruthenium(II) Complexes of 2,6-Dimethylpyrazine

Henrique E. Toma* and Eduardo Stadler

Received October 17, 1984

The pK_a of the coordinated pyrazine ion (pzH^+) has been used to estimate the back-bonding capability of a number of low-spin transition-metal complexes.[1,2] In this regard, the effective pK_a's of $[(CN)_5Ru(pzH)]^{2-}$ and $[(CN)_5Fe(pzH)]^{2-}$ have been recently determined by Johnson and Shepherd[3] as 0.4 and 0.065, respectively, being smaller than that for the coordinated pyrazine ligand (pK_a = 0.6). The extent of back-bonding in these complexes, based on MLCT and pK_a data, was reported to be 9% and 7%, respectively. However, as Johnson and Shepherd have pointed out, these data are not in harmony with the NMR results, which indicate that back-bonding to the pz ligand is more extensive for the $[(CN)_5Fe(pz)]^{3-}$ complex than for the $[(CN)_5Ru(pz)]^{3-}$ analogue.

In this work, we have extended the preceding basicity studies[3,4] to the 2,6-dimethylpyrazine (dmpz) complexes with $(CN)_5Fe^{3-}$, $(CN)_5Ru^{3-}$, and $(NH_3)_5Ru^{2+}$. Our choice was based on the fact that the dmpz ligand has a pK_a = 1.9,[5] comparable to that for the coordinated cyanide ligands in typical cyanoiron complexes.[4] Therefore, in contrast with the case of the pz complexes, the increase of basicity promoted by back-bonding interactions would be unambiguously detected by a preferential protonation of the dmpz ligand.

Experimental Section

Potassium hexacyanoruthenate(II) trihydrate (Alfa) and 2,6-dimethylpyrazine (Aldrich) were used as supplied. All other chemicals were reagent grade. The $[(NH_3)_5Ru(dmpz)](PF_6)_2$ and $K_3[Ru(CN)_5(dmpz)]$ complexes were synthesized according to literature procedures[1,3] for related compounds. Anal. Calcd for $RuC_6N_7H_{23}P_2F_{12}$: C, 12.33; N, 16.78; H, 3.96. Found: C, 12.2; N, 16.1; H, 4.1. Calcd for $K_3RuC_{11}N_7H_8(C_3H_6O)$: C, 32.67; N, 19.04; H, 2.74. Found: C, 33.2; N, 20.0; H. 3.0. The $[(CN)_5Fe(dmpz)]^{3-}$ complex was freshly prepared in aqueous solution by reacting $Na_3[Fe(CN)_5NH_3]\cdot 3H_2O$ with at least 5 times excess of dmpz to prevent the dissociation of the coordinated ligand. The complex was also isolated as a hygroscopic solid by precipitating with ethanol. The analyses were consistent with the composition $Na_3[Fe(CN)_5dmpz]\cdot 3H_2O$. Anal. Calcd: C, 31.68; N, 23.50; H, 3.38. Found: C, 30.7; N, 22.8; H, 3.5.

The electronic spectra were recorded on a Cary 14 or 17 spectrophotometer fitted with thermostated cell compartments. Potentiometric and pH measurements were made with a digital Orion 801-A instrument, using a combined glass–Ag/AgCl microelectrode. Cyclic voltammetry was carried out with a Princeton Applied Research instrument, consisting of a 173 potentiostat and a 174 universal programmer. Platinum or gold disk electrodes were employed for the measurements, using the conventional Luggin capillary with the Ag/AgCl (1 M KCl) reference electrode in a nonisothermic arrangement. A platinum wire was used as the auxiliary electrode.

The pK_a's of the complexes were determined independently by spectrophotometry and cyclic voltammetry as a function of pH. Cells specially designed for the experiments were used, combining simultaneous pH measurements with absorption spectra, or cyclic voltammetry, under nitrogen atmosphere.

Results and Discussion

The spectrum of the $[(NH_3)_5Ru(dmpz)]^{2+}$ complex is shown in Figure 1A. The strong absorption at 460 nm ($\epsilon = 8.0 \times 10^3$ M^{-1} cm^{-1}) is assigned to a metal-to-ligand charge transfer (MLCT) transition. An additional band centered at 267 nm (ϵ

(1) Ford, P.; Rudd, D. P.; Gaunder, R.; Taube, H. *J. Am. Chem. Soc.* **1968**, *90*, 1187–1194.
(2) Sen, J.; Taube, H. *Acta Chem. Scand., Ser. A* **1979**, *A33*, 125–135.
(3) Johnson, C. R.; Shepherd, R. E. *Inorg. Chem.* **1983**, *22*, 1117–1123.
(4) Toma, H. E.; Malin, J. M. *Inorg. Chem.* **1973**, *12*, 1039–1045.
(5) Chia, A. S.; Trimble, R. F., Jr. *J. Phys. Chem.* **1961**, *65*, 863–866.

0020-1669/85/1324-3085$01.50/0

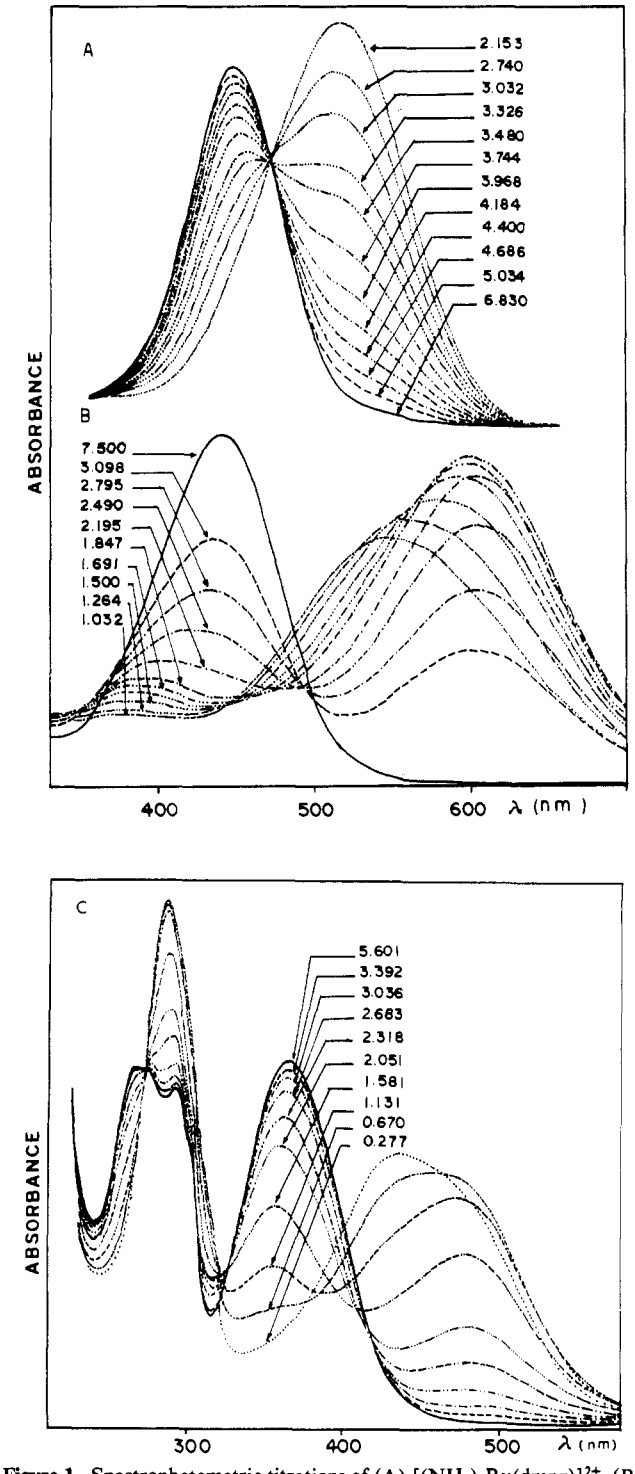

Figure 1. Spectrophotometric titrations of (A) $[(NH_3)_5Ru(dmpz)]^{2+}$, (B) $[(CN)_5Fe(dmpz)]^{3-}$, and (C) $[(CN)_5Ru(dmpz)]^{3-}$ with hydrochloric acid, at 25 °C; initial ionic strength = 0.10 M (NaCl). The pH values (±0.005) are indicated in the figure.

$= 5.1 \times 10^3\ M^{-1}\ cm^{-1}$) is assigned as an intraligand $\pi-\pi^*$ transition. Protonation of the $[(NH_3)_5Ru(dmpz)]^{2+}$ complex shifts the MLCT band to 530 nm with an isosbestic point at 483 nm. Analogously to the case of the $[(NH_3)_5Rupz]^{2+}$ complex,[1,3] the following equilibrium can be proposed:

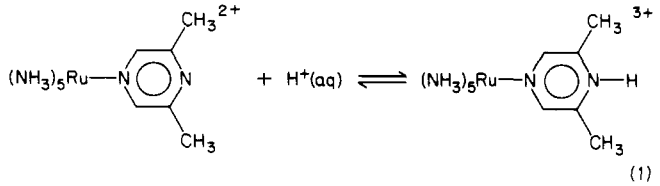

(1)

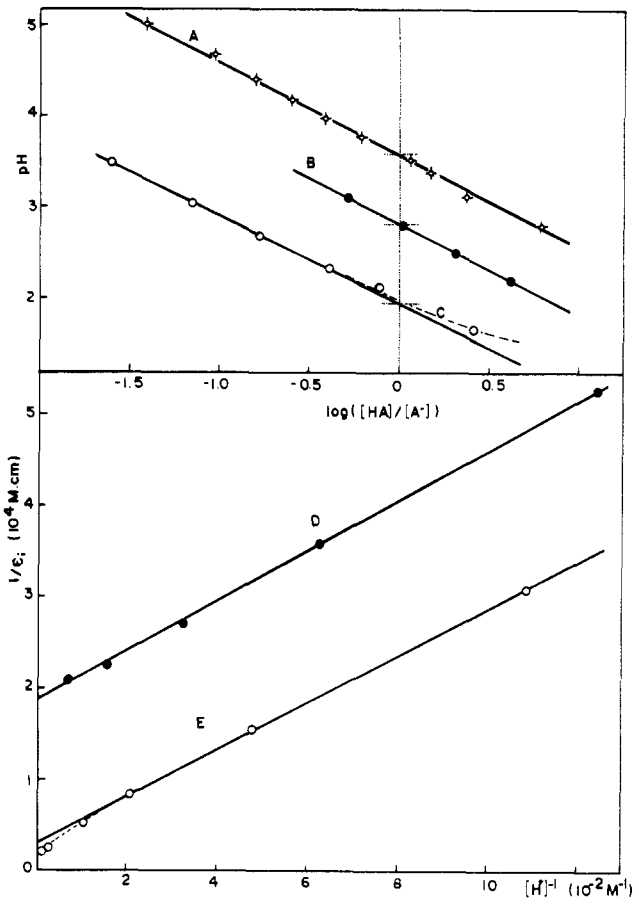

Figure 2. Determination of the pK_a's of dmpz complexes as described in the text: (A) $[(NH_3)_5Ru(dmpzH)]^{2+}$ at 528 nm; (B) $[HNC(CN)_4Fe(dmpz)]^{2-}$ at 600 nm; (C) $[(CN)_5Ru(dmpzH)]^{2-}$ at 288 nm; (D) $[HNC(CN)_4Fe(dmpz)]^{2-}$ + $[(CN)_5Fe(dmpzH)]^{2-}$ at 600 nm; (E) $[HNC(CN)_4Ru(dmpz)]^{2-}$ + $[(CN)_5Ru(dmpzH)]^{2-}$ at 478 nm.

The evaluation of the pK_a in this case is rather simple; however, instead of using the midpoint procedure in the plots of the relative absorbance changes ($\Delta A/\Delta A_{total}$) against pH, we preferred to use eq 2, where A_0 and A_f are the initial and final absorbances,

$$pH = pK_a - \log \frac{[MLH^+]}{[ML]} = pK_a - \log \frac{A - A_0}{A_f - A} \qquad (2)$$

respectively. For a well-behaved system, the plots of pH vs. log $[(A - A_0)/(A_f - A)]$ are linear, with a unitary slope. The pK_a is obtained at the intercept with the ordinate axis. In the present case, $pK_a = 3.55 \pm 0.05$.

The A_f values are often influenced by successive equilibria and many other sources of errors. As A_f approaches the ideal value, the slope tends to unity. Therefore, eq 2 provides a simple way of evaluating A_f in more complicated systems, such as the cyanometalates.

In the case of the $[(CN)_5Fe(dmpz)]^{3-}$ complex, the MLCT band at 440 nm ($\epsilon = 5.0 \times 10^3\ M^{-1}\ cm^{-1}$) decays, systematically, from pH 7 to 2, with a parallel growth of a new band, at 600 nm, assigned to the $[(CN)_5Fe(dmpzH)]^{2-}$ complex. An isosbestic point is roughly defined at 493 nm, as shown in Figure 1B, being an evidence that protonation on the pyrazine ligand predominates in this pH range.

A treatment based on eq 2 led to a slope smaller than unity. The explanation is that the A_f value based on the maximum absorbance at 600 nm is influenced by the competitive protonation on the cyanides. By an iterative procedure on the A_f values, the pK_a of $[(CN)_5Fe(dmpzH)]^{2-}$ was evaluated as 2.80 ± 0.05, as shown in Figure 2B.

In order to evaluate the contribution of the $[HNC(CN)_4Fe(dmpz)]^{2-}$ species (HML) in the equilibrium mixture, we have performed a careful analysis of the spectophotometric data considering reactions 3 and 4.

$$(CN)_5Fe(dmpz)^{3-} + H^+(aq) \rightleftharpoons (CN)_5Fe(dmpzH)^{2-} \quad (3)$$

$$(CN)_5Fe(dmpz)^{3-} + H^+(aq) \rightleftharpoons HNC(CN)_4Fe(dmpz)^{2-} \quad (4)$$

At 600 nm only the $[(CN)_5Fe(dmpzH)]^{2-}$ complex absorbs. Therefore, for a 1-cm optical path length, the measured absorbance, A_m, is given by eq 5. The total concentration of the metal

$$A_m = \epsilon_{MLH}[MLH] \quad (5)$$

complex, in the pH range from 7 to 2, can be represented by eq 6.

$$[M_{total}] = [ML] + [MLH] + [HML] \quad (6)$$

The quotient $[M_{total}]/A_m$ can be obtained from eq 5 and 6, after substituting the concentrations of the several species by the equilibrium expressions:

$$\frac{[M_{total}]}{A_m} = \frac{K_{MLH} + K_{HML}}{\epsilon_{MLH}K_{MLH}} + \frac{1}{\epsilon_{MLH}K_{MLH}}\frac{1}{[H^+]} \quad (7)$$

The plots of $[M_{total}]/A_m$ against $[H^+]^{-1}$ were linear, as shown in Figure 2D. From the slope and intercept we obtained

$$\epsilon_{MLH}K_{MLH} = 3.7 \times 10^6\ M^{-2}\ cm^{-1} \quad (8)$$

$$K_{MLH} + K_{HML} = 700\ M^{-1} \quad (9)$$

Substitution of $K_{MLH} = 600\ M^{-1}$ into eq 9 leads to K_{HML}, the protonation constant of $[HNC(CN)_4Fe(dmpz)]^{2-}$, equal to 100 M^{-1}.

For the $[(CN)_5Ru(dmpz)]^{3-}$ complex, the MLCT band at 364 nm ($\epsilon = 7.7 \times 10^3\ M^{-1}\ cm^{-1}$) decays systematically from pH 6 to 2, as shown in Figure 2, with a parallel growth of a new band at 478 nm, assigned to the $[(CN)_5Ru(dmpzH)]^{2-}$ complex. The lack of isosbestic point in the visible region indicates that the formation of $[HNC(CN)_4Ru(dmpz)]^{2-}$ species is strongly competitive in this case.

The plots of $[M_{total}]/A_m$ against $[H^+]^{-1}$ are linear, as shown in Figure 2E. Below pH 1.5, however, there is an increasing deviation from linearity, due to the formation of diprotonated species. From the slope and intercept we have obtained $\epsilon_{MLH}K_{MLH} = 3.9 \times 10^5\ M^{-2}\ cm^{-1}$ and $K_{MLH} + K_{HML} = 120\ M^{-1}$.

Because of the strong equilibrium overlap between $[(CN)_5Ru(dmpzH)]^{2-}$, $[(HNC)(CN)_4Ru(dmpz)]^{2-}$ and $[HNC(CN)_4Ru(dmpzH)]^-$ species, the procedure based on eq 2 cannot be used to evaluate K_{MLH} in the same way as for the cyanoiron complex.

Analogously to the case of the complexes investigated by Johnson and Shepherd,[3] there is a well-defined isosbestic point in the ultraviolet region (Figure 1C). This kind of behavior arises from the fact that the absorption band associated with the intraligand (dmpz) $\pi-\pi^*$ transition is not sensitive to protonation on cyanide and changes only when the coordinated pyrazine is protonated.[3] In this case $\epsilon_{ML} = \epsilon_{HML}$ and $\epsilon_{MLH} = \epsilon_{HMLH}$.

Considering the equilibria

$$\begin{array}{ccc} (CN)_5Ru(dmpz)^{3-} + H^+(aq) & \overset{K_{MLH}}{\rightleftharpoons} & (CN)_5Ru(dmpzH)^{2-} \\ \Big\downarrow\!\uparrow K_{HML} & & \Big\downarrow\!\uparrow K'_{HMLH} \\ HNC(CN)_4Ru(dmpz)^{2-} + H^+(aq) & \overset{K_{HMLH}}{\rightleftharpoons} & HNC(CN)_4Ru(dmpzH)^- \end{array} \quad (10)$$

for the pH range from 6 to 1, the total concentration of ruthenium(II) complex is given by

$$[M_{total}] = [ML] + [MLH] + [HML] + [HMLH] \quad (11)$$

The absorbances can be expressed by

$$A_0 = \epsilon_{ML}[M_{total}] \quad (12)$$

$$A_f = \epsilon_{MLH}[M_{total}] \quad (13)$$

$$A = \epsilon_{ML}([ML] + [HML]) + \epsilon_{MLH}([MLH] + [HMLH]) \quad (14)$$

By use of the equilibrium expressions, eq 14 can be converted in

$$\frac{A - A_0}{A_f - A} = \frac{K_{MLH}[H^+] + K_{HML}K_{HMLH}[H^+]^2}{1 + K_{HML}[H^+]} \quad (15)$$

Table I. Spectral and pK_a Data for 2,6-Dimethylpyrazine Complexes

complex	MLCT abs, 10^{-3} cm^{-1} unproton.	proton.	pK_a(gs)	pK_a*	ref
dmpzH$^+$			1.90		5
			1.94		this work
$(NH_3)_5Ru$-(dmpzH)$^{3+}$	21.74	18.94	3.70		this work[a]
	21.74	18.94	3.55	9.5	this work[b]
	21.74	18.94	3.40		this work[c]
$(CN)_5Fe(dmpzH)^{2-}$	22.72	16.66	2.80	15.5	this work[b]
$HNC(CN)_4Fe$-(dmpz)$^{2-}$	22.72	25.64	2.00		this work[b]
$HCN(CN)_4Fe$-(dmpzH)$^-$		18.52	1.5		this work[d]
$(CN)_5Ru(dmpzH)^{2-}$	27.47	20.92	1.90	15.6	this work[b]
$HNC(CN)_4Ru$-(dmpz)$^{2-}$	27.47	28.17	1.60		this work[b]
$HNC(CN)_4Ru$-(dmpzH)$^-$		23.0	<1		this work[b]
pzH$^+$			0.65		5
$(NH_3)_5Ru(pzH)^{3+}$	21.18	18.90	2.5	7.3	1
			2.85		3
$(NH_3)_5Os(pzH)^{3+}$	21.74	23.36	7.4	3.8	2

[a] 15 °C. [b] 25 °C. [c] 35 °C. [d] Based on cyclic voltammetry.

When a single equilibrium predominantes, eq 15 becomes identical with eq 2. Therefore, a plot of pH vs. log $[(A - A_0)/(A_f - A)]$ would be linear, with a unitary slope. When two successive equilibria take place, the remaining terms in eq 15 would lead to an increasing deviation from linearity, as shown in Figure 2C. In the present case, the pK_{MLH} can be easily obtained by extrapolating the linear part with unitary slope, as illustrated in the figure. By combining the results from Figure 2C,E, we have evaluated the individual equilibrium constants, $K_{MLH} = 80\ M^{-1}$ and $K_{HML} = 40\ M^{-1}$, and also $\epsilon_{MLH} = 4.9 \times 10^3\ M^{-1}\ cm^{-1}$, at 487 nm.

Table I summarizes the spectroscopic and equilibrium constants obtained in this work for the 2,6-dimethylpyrazine complexes of $Ru(NH_3)_5^{2+}$, $(CN)_5Fe^{3-}$, and $(CN)_5Ru^{3-}$.

Cyclic Voltammetry. The cyclic voltammograms of the $[(NH_3)_5Ru(dmpz)]^{2+}$ and $[(CN)_5Fe(dmpz)]^{3-}$ complexes were essentially reversible, with separation of the anodic and cathodic peaks within 60–70 mV and current ratios very close to unity. The half-wave potentials for these complexes were 0.465 and 0.537 V vs. NHE, respectively.

Protonation of the dmpz complexes leads to systematic anodic shifts in the cyclic voltammograms, as shown in Figure 3A,B. For the $[(NH_3)_5Ru(dmpz)]^{2+}$ complex, the plots of $E_{1/2}$ against pH (Figure 3C) are linear, up to pH 3, with a slope close to 60 mV/pH. From the intersection with the parallel line, the pK_a of the dmpz complex was evaluated as 3.6 ± 0.1, in excellent agreement with the spectrophotometric data.

For the $[(CN)_5Fe(dmpz)]^{3-}$ complex, the plots of $E_{1/2}$ against pH (Figure 3D) can be fitted by two straight lines of slopes close to 60 and 120 mV/pH, corresponding to one- and two-proton processes, respectively.[6] The first pK_a (=2.9 ± 0.1) was ascribed to the $[(CN)_5Fe(dmpzH)]^{2-}$ and $[HNC(CN)_4Fe(dmpz)]^{2-}$ complexes and is comparable to those obtained spectrophotometrically. The second pK_a (=1.5 ± 0.2) was ascribed to the diprotonated species $[HNC(CN)_4Fe(dmpzH)]^-$.

The electrochemical behavior of the $[(CN)_5Ru(dmpz)]^{2-}$ complex was quasi-reversible, with $E_{1/2} \cong 1.2$ V vs. NHE. Anodic shifts were observed for the cyclic voltammograms below pH 2; however, systematic measurements were precluded by an increasingly poor electrochemical response and by the voltage limit in aqueous solution.

(6) Wawzonek, S. "Physical Methods of Chemistry"; Weissberger, A., Rossiter, B. W., Eds.; Wiley-Interscience: New York, 1971; Part IIA, Chapter 1.
(7) Jackson, G.; Porter, G. *Proc. R. Soc. London, Ser. A* **1961**, *260*, 13–30.

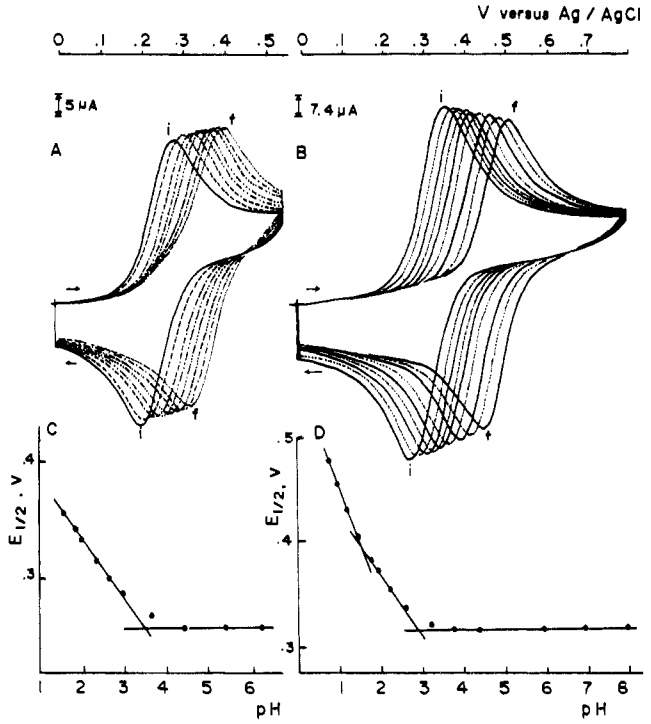

Figure 3. Cyclic voltammograms of the (A) $[(NH_3)_5Ru(dmpz)]^{2+}$ and (B) $[(CN)_5Fe(dmpz)]^{3-}$ complexes from pH 8 to 1.58 and from pH 8 to 0.70 (i-f), respectively, with the corresponding plots of $E_{1/2}$ vs. pH ([NaCl] = 0.10 M, 25 °C).

Excited-State pK_a. Calculation of the pK_a* of each complex was carried out by using eq 16,[1,7] where pK_a(gs) is the ground-state

$$pK_a^* = pK_a(gs) + 2.86(\nu_1 - \nu_2)/RT \qquad (16)$$

pK_a, ν_1 is the frequency in wavenumbers of the absorption band of the unprotonated form, and ν_2 is the frequency of the corresponding absorption band in the protonated form. The results are shown in Table I.

The pK_a* values of the cyanometalates are 6 orders of magnitude higher than that of the ruthenium(II)-ammine analogue. The difference may be associated with the metal-ligand interactions in the excited states; however, there are two additional points to be considered in the present system. The MLCT transition energies used in eq 16 are strongly dependent on the potential diagrams, so that the differences of nuclear configuration between the ground and excited states of ML and MLH would increase the calculated pK_a*. The second point is that, in the derivation of eq 16, the entropy changes for the ground- and excited-state reactions have been considered the same. This kind of approximation may be reasonable for ruthenium(II) ammines and related complexes; however, it seems unlikely for the cyanometalates, which are very strongly dependent on solvent interactions.[8]

Conclusion

The basicity of the $[(CN)_5Fe(dmpz)]^{3-}$ and $[(NH_3)_5Ru(dmpz)]^{2+}$ complexes increases, respectively, by 1 and 2 orders of magnitude with respect to the free dmpz ligand (Table I). The pK_a of the $[(CN)_5Ru(dmpz)]^{3-}$ complex is similar to that of dmpz. Therefore, the extent of metal-to-ligand back-bonding, based on the relative pK_a values, increases along the series

$$Ru(CN)_5L^{3-} < Fe(CN)_5L^{3-} < Ru(NH_3)_5L^{2+}$$

in agreement with the NMR work reported by Johnson and Shepherd, for the related pz complexes.[9] Protonation on the cyanides decreases the pK_a of the coordinated dmpz ligand. Since the pK_a of $[HNC(CN)_4Fe(pz)]^{2-}$ is 1.9,[4] the pK_a of 0.065 measured by Johnson and Shepherd[3] should be ascribed to the diprotonated species $[HNC(CN)_4Fe(pzH)]^-$, rather than to $[(CN)_5Fe(pzH)]^{2-}$.

Registry No. dmpz, 108-50-9; $[(CN)_5Fe(dmpz)]^{3-}$, 97431-16-8; $[(CN)_5Ru(dmpz)]^{3-}$, 97431-17-9; $[(NH_3)_5Ru(dmpz)]^{2+}$, 97431-18-0.

(8) Toma, H. E.; Takasugi, M. S. *J. Solution Chem.* **1983**, *8*, 547-561.
(9) Johnson, C. R.; Shepherd, R. E. *Inorg. Chem.* **1983**, *22*, 2439-2444.

Contribution from the Departments of Chemistry and Chemistry Education, Seoul National University, Seoul 151, Korea

Kinetics of the Metal Ion Catalyzed Ester Hydrolysis of *O*-Acetyldi-2-pyridyl Ketoxime

Junghun Suh,*† Myunghyun Paik Suh,‡ and Jae Don Lee†

Received January 23, 1985

Kinetic studies on the metal ion catalyzed reactions of acyl derivatives disclosed various catalytic features.[1,2] In addition, possible catalytic roles of metal ions in metalloenzymes were proposed from these studies. Previous investigation on the metal ion catalyzed ester hydrolysis of the acetyl esters (**1**, **2**) of pyridyl

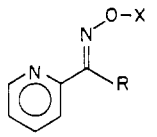

A

1: X = $\overset{O}{\overset{\|}{C}}CH_3$, R = H
1a: X = H, R = H
2: X = $\overset{O}{\overset{\|}{C}}CH_3$, R = CH_3
2a: X = H, R = CH_3
3: X = $\overset{O}{\overset{\|}{C}}CH_3$, R = 2-pyridyl
3a: X = H, R = 2-pyridyl

oximes **1a** and **2a** established the mechanism of B.[3-6] In this

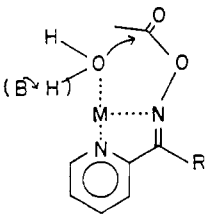

B

R = H or CH_3
M = Zn(II) or Cu(II)

mechanism, the metal-bound water molecule or hydroxide ion makes a nucleophilic attack at the complexed ester linkage. Support for this mechanism came from the reactivity-selectivity relationship,[4] steric acceleration by the methyl substituent in **2**,[5] and the bimolecular participation of hydroxozinc(II) ion in the hydrolysis of **2**.[5]

We have extended the study to *O*-acetyldi-2-pyridyl ketoxime (**3**), in an attempt to gain further insight into the nature of the steric compression[5] in the metal ion catalyzed hydrolysis of the oxime esters. Ester **3** is the only analogue of **1** and **2** to which

† Department of Chemistry.
‡ Department of Chemistry Education.

0020-1669/85/1324-3088$01.50/0